Pramana – J. Phys. (2017) 89:43
DOI 10.1007/s12043-017-1445-5

Matter density distributions and elastic form factors of some two-neutron halo nuclei

AHMED N ABDULLAH

Department of Physics, College of Science, University of Baghdad, Baghdad, Iraq
E-mail: Ahmednajim@scbaghdad.edu.iq

MS received 24 November 2016; revised 8 May 2017; accepted 12 May 2017; published online 31 August 2017

Abstract. The Skyrme–Hartree–Fock (SHF) method with MSK7 Skyrme parameter has been used to investigate the ground-state properties for two-neutron halo nuclei ^{6}He, ^{11}Li, ^{12}Be and ^{14}Be. These ground-state properties include the proton, neutron and matter density distributions, the corresponding rms radii, the binding energy per nucleon and the charge form factors. These calculations clearly reveal the long tail characterizing the halo nuclei as a distinctive feature.

Keywords. Halo nuclei; elastic electron scattering.

PACS Nos 21.10.Gv; 25.30.Bf

1. Introduction

The investigation of the structure of nuclei far from the β stability line is one of the most interesting subjects in nuclear physics. The use of the radioactive nuclear beam (RNB) offers a good opportunity to study the properties of nuclei far from the β stability line. Many new progresses have been made in recent years. The discovery of halo phenomena in exotic nuclei is one of the typical examples. In general, the halo nucleus has large neutron excess or proton excess where a few outside nucleons are very weakly bound. Such halo systems are well described by the few-body models, which assume that halo nuclei consist of a core and a few outside nucleons. The small separation energy of the last nucleon, the extended density distribution and the narrow momentum distribution due to the Heisenberg uncertainty principle are important properties of halo nucleus. In this case, the nuclear structure models based on the experimental data for stable nuclei should be improved and new theoretical models to describe the special structure of nuclei far from the β stability line are required [1].

Most exotic nuclei are so short lived that they cannot be used as targets at rest. Instead, direct reactions with RNB can be done in inverse kinematics, where the role of the beam and the target are interchanged [2].

Zukav and Thompson [3] discussed the proton dripline nucleus ^{17}Ne in a three-body model of ^{15}O plus two protons. The calculations showed that the ^{17}Ne nucleus has a Borromean structure, and a matter rms radius of 2.77–2.81 fm, which is in agreement with experimental data. Antonov *et al* [4] calculated and compared charge form factors corresponding to proton density distributions in exotic nuclei, such as ^{6,8}He and ^{11}Li, ^{17,19}B and ^{14}Be. The result of such a comparison would show the effect of the neutron halo or skin on the proton distributions in exotic nuclei.

The aim of this research is to examine the validity of the Skyrme–Hartree–Fock (SHF) model to study the nuclear structures of the halo nuclei. For this, the ground-state proton, neutron and matter density distributions, corresponding rms and the charge form factors for two neutrons halo nuclei ^{6}He, ^{11}Li, ^{12}Be and ^{14}Be have been calculated using MSK7 [5] Skyrme parameter and the obtained results are compared with the corresponding available experimental data.

2. Theory

The conventional Skyrme force is the most suitable force to describe the ground-state properties of nuclei. This force basically consists of a two-body term and a three-body term [6]:

$$V_{\mathrm{CS}} = \sum_{i<j} V_{ij}^{(2)} + \sum_{i<j<k} V_{ijk}^{(3)} \tag{1}$$

with

$$V_{ij}^{(2)} = t_0(1 + x_0 p_\sigma)\delta(\vec{r}) + \frac{1}{2}t_1[\delta(\vec{r})\vec{k}^2 + \vec{k'}^2\delta(\vec{r})] + t_2\vec{k'} \cdot \delta(\vec{r})\vec{k} + iW_0(\vec{\sigma}_i - \vec{\sigma}_j) \cdot \vec{k} \times \delta(\vec{r})\vec{k}, \quad (2)$$

$$V_{ijk}^{(3)} = t_3\delta(\vec{r}_i - \vec{r}_j)\delta(\vec{r}_j - \vec{r}_k). \quad (3)$$

The three-body term in eq. (1) can be replaced by a density-dependent two-body term [7]:

$$V_{ijk}^{(3)} \cong V_{ij}^{(2)} = \frac{1}{6}t_3\rho(\vec{R})\delta(\vec{r}), \quad (4)$$

where

$$\vec{R} = (\vec{r}_i + \vec{r}_j)/2 \quad \text{and} \quad \vec{r} = (\vec{r}_i - \vec{r}_j),$$

the relative momentum operators $\hat{k} = (\nabla_i - \nabla_j)/2i$ and $\hat{k'} = -(\nabla_i - \nabla_j)/2i$ are acting to the right and to the left, respectively [6].

The Skyrme forces, with the three-body term replaced by a density-dependent two-body term, are unified in a single form by Ge *et al* [8] as an extended Skyrme force:

$$\begin{aligned} V_{\text{Skyrme}} = \sum_{i<j} V_{ij} &= t_0(1 + x_0 P_\sigma)\delta(\vec{r}) \\ &+ \frac{t_1}{2}(1 + x_1 P_\sigma)[\delta(\vec{r})\vec{k}^2 + \vec{k'}^2\delta(\vec{r})] \\ &+ t_2(1 + x_2 P_\sigma)\vec{k'} \cdot \delta(\vec{r})\vec{k} \\ &+ \frac{1}{6}t_3(1 + x_3 P_\sigma)\rho^\alpha(\vec{R})\delta(\vec{r}) \\ &+ it_4\vec{k'} \cdot \delta(\vec{r})(\vec{\sigma}_i + \vec{\sigma}_j) \times \vec{k}, \end{aligned} \quad (5)$$

where P_σ is the space exchange operator, $\delta(\vec{r})$ is the delta function, $\vec{k}$ is the relative momentum, $\vec{\sigma}$ is the vector of Pauli spin matrices and t_0, t_1, t_2, t_3, t_4, x_0, x_1, x_2, x_3, and α are Skyrme force parameters.

In the SHF method the proton, neutron or charge densities are given by [9]

$$\rho_k(\vec{r}) = \sum_{\beta \in k} w_\beta \psi_\beta^+(\vec{r})\psi_\beta(\vec{r}), \quad (6)$$

where k denotes the proton or neutron, ψ_β is the single-particle wave function of the state β and w_β represents the occupation probability of the state β.

The root mean square (rms) radii of the neutron, proton and charge distributions can be obtained from these densities as follows [6]:

$$r_k = \langle r_k^2 \rangle^{1/2} = \left[\frac{\int r^2\rho_k(r)\mathrm{d}r}{\int \rho_k(r)\mathrm{d}r}\right]^{1/2}, \quad k = n, p, c. \quad (7)$$

The total charge form factor squared for unpolarized electrons and target is given by [10]

$$|F_{\text{ch}}(q)|^2 = |F_0(q)|^2 + |F_2(q)|^2. \quad (8)$$

The elastic charge form factor, $F_0(q)$, is calculated by the Fourier transform of the ground-state charge density distribution [10], i.e.

$$F_0(q) = \frac{4\pi}{Z}\int_0^\infty \rho_{0\text{ch}}(r)\, j_0(qr)\, r^2\mathrm{d}r, \quad (9)$$

where $j_0(qr)$ is the spherical Bessel function of order zero and q is the momentum transfer from the incident electron to the target nucleus.

The normalization of the ground-state charge density distributions, $\rho_{0\text{ch}}$, is given by [10]

$$Z = 4\pi\int_0^\infty \rho_{0\text{ch}}(r)r^2\mathrm{d}r. \quad (10)$$

The quadrupole form factor, $F_2(q)$, is obtained by the undeformed p-shell model as [10,11]

$$F_2(q) = \frac{\langle r^2 \rangle}{Q}\left(\frac{4}{5P_J}\right)^{1/2}\int \rho_{2\text{ch}}(r)\, j_2(qr)r^2\mathrm{d}r, \quad (11)$$

where $j_2(qr)$ is the second order of the spherical Bessel functions, Q is the quadrupole moment and P_J is a quadrupole projection factor given as [11]

$$P_J = \frac{J(2J-1)}{(J+1)(2J+3)}. \quad (12)$$

3. Results and discussion

The Skyrme–Hartree–Fock (SHF) method with MSK7 [5] parameter is employed to study the ground-state proton, neutron and matter densities and the associated root mean square (rms) radii of Borromean two-neutron halo nuclei ^{6}He (S_{2n} = 0.975 MeV, $\tau_{1/2}$ = 806 ms), ^{11}Li (S_{2n} = 369 keV, $\tau_{1/2}$ = 8.75 ms), ^{12}Be (S_{2n} = 3.67 MeV, $\tau_{1/2}$ = 20 ms) and ^{14}Be (S_{2n} = 1.27 MeV, $\tau_{1/2}$ = 4.35 ms) [12,13]. For completeness, the binding energy per nucleon and elastic charge form factors also are evaluated within the same framework.

The nucleus ^{6}He (J^π, $T = 0^+$, 1) is composed of a core ^{4}He (J^π, $T = 0^+$, 0) and two halo neutrons (J^π, $T = 0^+$, 1). The nucleus ^{11}Li (J^π, $T = 3/2^-$, 5/2) is composed of a core ^{9}Li (J^π, $T = 3/2^-$, 3/2) and two halo neutrons (J^π, $T = 0^+$, 1). The nucleus ^{12}Be (J^π, $T = 0^+$, 2) is composed of a core ^{10}Be (J^π, $T = 0^+$, 1) and two halo neutrons (J^π, $T = 0^+$, 1). The nucleus ^{14}Be (J^π, $T = 0^+$, 3) is composed of a core ^{12}Be (J^π, $T = 0^+$, 2) and two halo neutrons (J^π, $T = 0^+$, 1). The configurations $\{(1s_{1/2})^4\}$, $\{(1s_{1/2})^4, (1p_{3/2})^5\}$, $\{(1s_{1/2})^4, (1p_{3/2})^6\}$ and $\{(1s_{1/2})^4, (1p_{3/2})^6, (1p_{1/2})^2\}$ are assumed for core nuclei ^{4}He, ^{9}Li, ^{10}Be

Table 1. The calculated proton and neutron rms radii along with experimental results.

Nucleus	$\langle r_p^2\rangle^{1/2}$	$\langle r_p^2\rangle_{\rm exp}^{1/2}$ [14,15]	$\langle r_n^2\rangle^{1/2}$	$\langle r_n^2\rangle_{\rm exp}^{1/2}$ [15–17]	$\langle r_n^2\rangle^{1/2} - \langle r_p^2\rangle^{1/2}$
^{6}He	2.159	2.21 ± 0.03	2.996	2.87 ± 0.04	0.837
^{11}Li	2.264	2.37 ± 0.04	3.253	3.21 ± 0.17	0.989
^{12}Be	2.331	2.49 ± 0.06	2.946	2.75 ± 0.11	0.615
^{14}Be	2.335	–	3.659	3.68 ± 0.26	1.324

Table 2. The calculated charge, matter rms radii and the binding energy per nucleon along with experimental results.

Nucleus	$\langle r_c^2\rangle^{1/2}$	$\langle r_m^2\rangle^{1/2}$	$\langle r_m^2\rangle_{\rm exp}^{1/2}$ [17–19]	BE (MeV)	BE exp. [12] (MeV)
^{6}He	2.127	2.745	2.73 ± 0.04	4.020	4.878
^{11}Li	2.306	3.016	3.12 ± 0.16	4.664	4.155
^{12}Be	2.393	2.756	2.73 ± 0.05	5.750	5.720
^{14}Be	2.393	3.335	2.36 ± 0.19	4.868	4.994

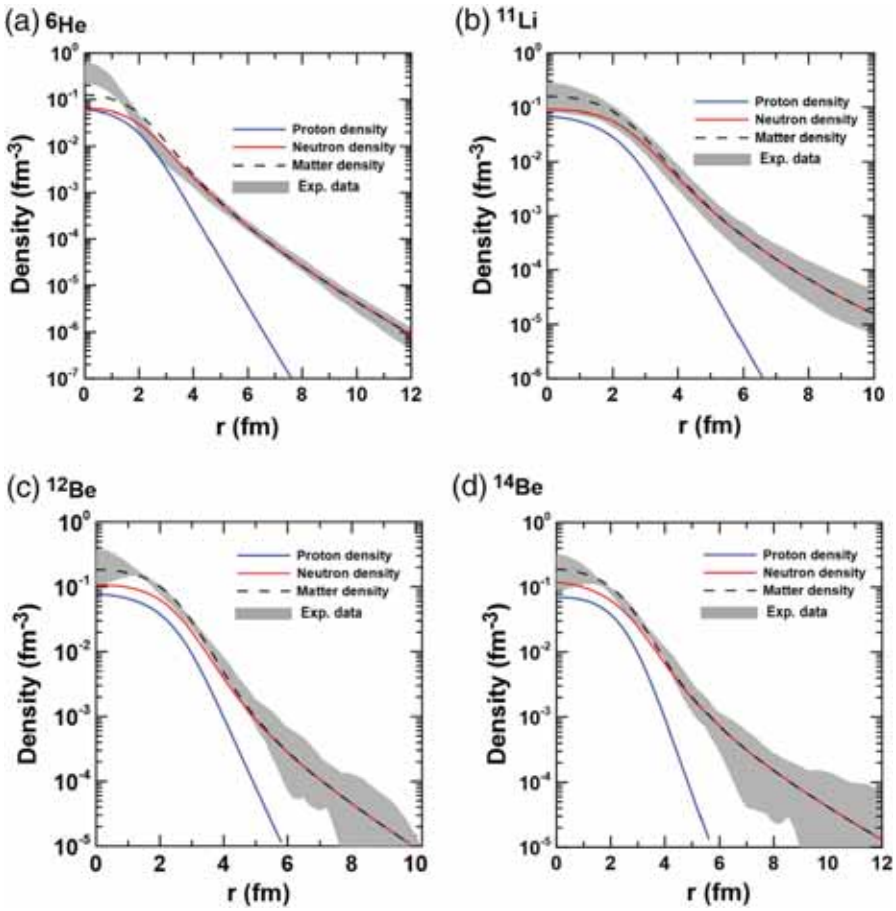

Figure 1. Proton, neutron and matter densities for ^{6}He, ^{11}Li, ^{12}Be and ^{14}Be halo nuclei compared with experimental data (the shaded area). The experimental data for ^{6}He and ^{11}Li are taken from ref. [14] while the experimental data for ^{12}Be and ^{14}Be are taken from ref. [19].

and ^{12}Be, respectively. The two halo neutrons in ^{6}He, ^{11}Li and ^{12}Be are assumed to be in a pure $1p_{1/2}$ orbit while those in ^{14}Be are considered in a pure $2s_{1/2}$ orbit.

The calculated proton, neutron, charge and matter rms radii and the binding energy per nucleon for ^{6}He, ^{11}Li, ^{12}Be and ^{14}Be halo nuclei using MSK7 Skyrme force

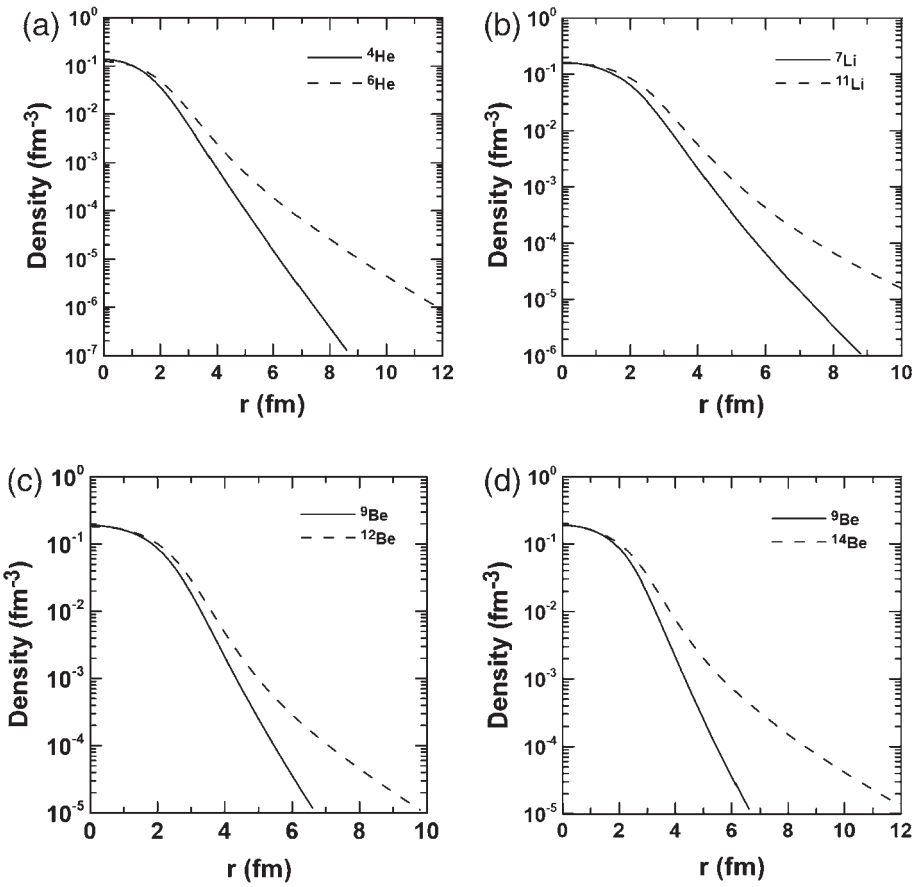

Figure 2. The comparison between the calculated matter density of unstable and stable nuclei.

parameters are arranged in tables 1 and 2 together with the corresponding experimental data. According to these results, the obtained values agree reasonably with the analogous experimental data for all nuclei under study.

The calculated proton, neutron and matter density distributions for ^{6}He, ^{11}Li, ^{12}Be and ^{14}Be halo nuclei using MSK7 Skyrme parameter are respectively displayed as blue, red and dashed curves in figure 1. The calculated densities in figures 1a, 1b, 1c and 1d correspond to ^{6}He, ^{11}Li, ^{12}Be and ^{14}Be halo nuclei, respectively. The experimental matter densities (denoted by the shaded area) [14,19] are shown in these figures for comparison. It is evident from these figures that the calculated matter density distributions agree well with the experimental data throughout the whole range of r. The long tail behaviour (considered as a distinctive feature of halo nuclei) is noticeably seen in the distribution of the neutron density. This behaviour is related to the existence of the outer two neutrons in the halo orbits. The calculated proton densities of the considered nuclei, shown in these figures, demonstrate steep slope behaviour because no protons are found in the halo orbits (all protons in these nuclei are found within their cores only). Besides, the difference between the calculated neutron and proton rms radii for interested halo nuclei is given in table 1. This difference gives a supplementary support for the halo structure of these nuclei.

Comparison of the matter density distributions of the unstable (halo) nuclei ^{6}He, ^{11}Li, ^{12}Be and ^{14}Be with those of the stable nuclei ^{4}He, ^{7}Li and ^{9}Be are displayed as dashed and solid curves, respectively in figure 2. The calculated matter density distributions in figures 2a, 2b, 2c and 2d correspond to pairs of (^{6}He, ^{4}He), (^{11}Li, ^{7}Li), (^{12}Be, ^{9}Be) and (^{14}Be, ^{9}Be) nuclei, respectively. It is clear from this figure that the matter density distributions of unstable nuclei and stable nuclei are diverse. As the outer two-neutron halos in ^{6}He, ^{11}Li, ^{12}Be and ^{14}Be nuclei are weakly bound, the matter density distributions of these nuclei have a longer tail than that of ^{4}He, ^{7}Li and ^{9}Be nuclei. Figures 1 and 2 give the conclusion that the halo phenomenon in ^{6}He, ^{11}Li, ^{12}Be and ^{14}Be is connected to the outer two neutrons but not to the core nucleons.

To illustrate the effect of long tail behaviour of the matter density distribution for neutron-rich nuclei on the charge form factors, the charge form factors (C0 + C2) for unstable nucleus ^{11}Li and that of stable nucleus ^{7}Li are calculated using MSK7 parameter and shown in

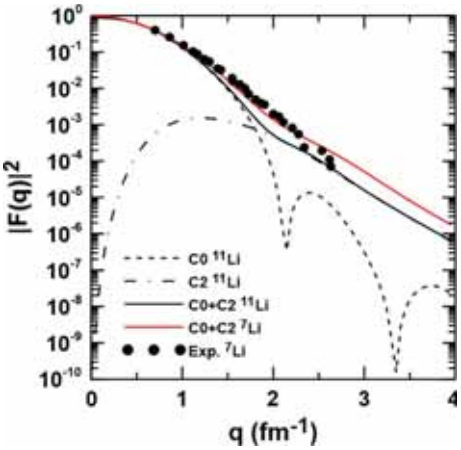

Figure 3. Dependence of the charge form factors on q for ^{7}Li and ^{11}Li nuclei using MSK7 parameter.

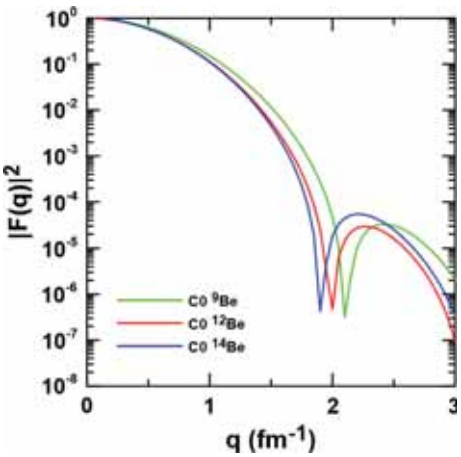

Figure 4. The comparison of the calculated elastic charge form factors of the unstable nuclei ^{12}Be and ^{14}Be with that of the stable nucleus ^{9}Be using MSK7 parameter.

figure 3. The quadrupole form factor contribution (C2) is obtained by the undeformed p-shell model. For comparison, the experimental data [11] of the charge form factors of the stable nucleus ^{7}Li are given in this figure. It is obvious from this figure that the calculated charge form factors of unstable nucleus decrease faster than that of the stable nucleus; this is due to the coupling of the additional four neutrons for the ^{11}Li nucleus with the ^{7}Li core which lead to a difference in the centre of mass correction.

Figure 4 exemplifies the comparison between the calculated elastic C0 charge form factors of the unstable (halo) nuclei ^{12}Be (red curve) and ^{14}Be (blue curve) and that of stable nucleus ^{9}Be (green curve) calculated by MSK7 parameter. It is clear from this figure that the calculated form factors of ^{9}Be, ^{12}Be and ^{14}Be isotopes have one diffraction minimum throughout all ranges of considered momentum transfer. In addition, the location of the minimum value has backward shift with increasing number of the neutrons. This change is due to the enhancement of proton densities in the peripheral region and also to the contribution of the charge distribution of the neutrons themselves.

4. Summary and conclusions

The ground-state proton, neutron and matter density distributions, the corresponding rms radii, the binding energy per nucleon and the elastic electron scattering form factors of two-neutron halo nuclei ^{6}He, ^{11}Li, ^{12}Be and ^{14}Be are studied by the SHF method with MSK7 Skyrme parameter. The calculated results are compared with the experimental data. The long tail behaviour, considered as a distinctive feature of halo nuclei, is evidently revealed in the calculated neutron and matter density distributions of nuclei under study. Besides, noticeable difference is found between the calculated overall proton and neutron rms radii of these nuclei which also indicates a halo structure. It is concluded that the SHF method with MSK7 Skyrme parameter is capable of reproducing information about the nuclear structures of the halo nuclei as do those of the experimental data.

References

[1] G Jun, J H Qing, L J Ye, Z Wei, R Z Zhou and L X Guo, *Commun. Theor. Phys.* **40**, 577 (2003)
[2] A N Antonov, D N Kadrev, M K Gaidarov, E M Guerra, P Sarriguren, J M Udias, V K Lukyanov, E V Zemlyanaya and G Z Krumova, *Phys. Rev. C* **72**, 044307 (2005)
[3] M V Zukov and I J Thompson, *Phys. Rev. C* **52**, 3505 (1995)
[4] A N Antonov, M K Gaidarov, D N Kadrev, P E Hodgson and E M Guerra, *Int. J. Mod. Phys. E* **13**, 759 (2004)
[5] S Goriely, F Tondeur and J M Pearson, *At. Data Nucl. Data Tables* **77**, 311 (2001)
[6] G Q Li, *J. Phys. G. Nucl. Part. Phys.* **17**, 1 (1991)
[7] D Vautherin and D M Brink, *Phys. Rev. C* **5**, 626 (1972)
[8] L X Ge, Y Z Zhuo and W Norenberg, *Nucl. Phys. A* **459**, 77 (1986)
[9] P G Reinhard, F Hummer and K Goeke, *Z. Phys. A* **317**, 339 (1984)
[10] T Stovall, J Goldemberg and D B Isabelle, *Nucl. Phys.* **86**, 225 (1966)
[11] L R Suelzle, M R Yearian and H Crannell, *Phys. Rev.* **162**, 992 (1967)
[12] M Wang, G Audi, A H Wapstra, F G Kondev, M M Cormick, X Xu and B Pfeiffer, *Chin. Phys. C* **36**, 1603 (2012)

[13] G Audi, F G Kondev, M Wang, B Pfeiffer, X Sun, J Blachot and M M Cormick, *Chin. Phys. C* **36**, 1157 (2012)
[14] I Tanihata, H Savajols and R Kanungo, *Prog. Part. Nucl. Phys.* **68**, 215 (2013)
[15] I Tanihata, T Kobayashi, O Yamakawa, S Shimoura, K Ekuni, K Sugimoto, N Takahashi, T Shimoda and H Sato, *Phys. Lett. B* **206**, 592 (1988)
[16] Y S Shen and Z Z Ren, *Phys. Rev. C* **54**, 1158 (1996)
[17] I Tanihata, H Hamagaki, O Hashimoto, S Nagamiya, Y Shida, N Yoshikawa, O Yamakawa, K Sugimoto, T Kobayashi, D E Greiner, N Takahashi and Y Nojiri, *Phys. Rev. Lett.* **55**, 2676 (1985)
[18] A Ozawa, T Suzuki and I Tanihata, *Nucl. Phys. A* **693**, 32 (2001)
[19] S Ilieva *et al*, *Nucl. Phys. A* **875**, 8 (2012)